JOTCSA Journal of the Turkish Chemical Society Section: A Chemistry

TURKISH CHEMICAL SOCIETY

Development of a Silica-Organic Framework Ionic Solid Bronsted Acid Catalyst for the Synthesis of 2,4,5-trisubstituted Imidazole Derivatives

Noor Abbas Alshook[1], Haitham Dalol Hanoon[1*], Hayder Hamied Mihsen[1]

[1]University of Karbala, Collage of Science, Department of Chemistry, Karbala, Iraq.

Abstract: Heterogeneous Bronsted acid is one of the most promising compounds that can be used as a catalyst in chemical production, and that can certainly have a positive impact on the environment. This research includes the preparation of heterogeneous Bronsted acid by using rice hulls as a starting material. The prepared acid was characterized by FTIR, XRD, TGA, SEM-EDX, TEM, and elemental analysis. The FTIR results showed the presence of N-H and S=O absorption bands within the expected range in prepared Bronsted acid. The specific surface area of the catalyst determined by Brunauer-Emmett-Teller (BET) using the nitrogen adsorption method is 205.42 m^2/g, and the average pore diameters are 3.69 nm, 2,4,5-Trisubstituted imidazole derivatives were prepared by reacting substituted aldehydes with benzil and ammonium acetate in the presence of a solid acid catalyst. The main advantages of this method are safe, cheap, and short reaction conditions. In addition, the prepared catalyst can be reused.

Keywords: Rice husks, Heterogeneous solid acid, Catalyst, Brønsted acid, Imidazole derivatives, Aldehydes.

Submitted: July 12, 2024. **Accepted:** December 19, 2024.

Cite this: Alshook NA, Hanoon HD, Mihsen HH. Development of a Silica-Organic Framework Ionic Solid Bronsted Acid Catalyst for the Synthesis of 2,4,5-trisubstituted Imidazole Derivatives. JOTCSA. 2025;12(1): 1-14.

DOI: https://doi.org/10.18596/jotcsa.1515088

***Corresponding author's E-mail:** haitham.alshebly@uokerbala.edu.iq

1. INTRODUCTION

Agricultural and industrial waste negatively impacts the environment by causing air pollution and contaminating water and soil. However, these issues can be mitigated by utilizing this waste, providing a potential source of income and a means to reduce waste production and its environmental effects (1). One of the essential agricultural wastes is rice husks, which are used in the composition of many medical and agricultural industries. They are the hard covering surrounding the grain of rice to protect it from insects and pathogens during growth. It is separated when the rice is harvested (2,3). Rice represents a significant food source for more than half of the Earth's population, with its annual volume reaching more than 100 million tons. Rice husks are rich in silica, or silicon dioxide, and represent about 20% of their weight. It is one of the common forms of silica found in nature, as it is rarely seen in its pure form (4,5). Notably, rice hulls have been talked about as a source of silica before. Last year, researchers at "Chaudhary Sharan" University in India published a similar study that concluded that rice husks represent a good source for obtaining silica with the appropriate structure at a low cost (6). Silica is obtained from the rice hulls as sodium silicate. So, acid treatment converts the silica into a gel. This method of extraction is possible at ambient temperatures and is an alternative to temperature treatment (7-9).

Sulfated silicate catalysts are comprised of two components: one is composed of sulfuric acid adsorbed to silica, and the other is composed of sulfated silica. The utilization of Sulfuric acid adsorbed on silica is simple and cost-effective for large-scale synthesis because the acid can be repeated without altering the catalytic system's activity. Studies have demonstrated that it is a safe, environmentally friendly, and reusable catalyst (10, 11). The adsorbed form of sulfuric acid on silica is considered an exceptional candidate for use as a chemical solvent or component of a chemical solution; the approach circumvents these limitations. Other chemicals, including silica acid, have been employed to catalyze chemical reactions to increase yields and other properties. Other common chemicals used to accomplish this include sulfuric acid and tribufos. Many research groups have employed this catalyst, which is composed of sulfonic

acid, as a powerful chemical reagent, such as silica sulfuric acid and solid sulfanilic acid (11, 12).

Solid acid catalysts synthesize many organic compounds, including heterocyclic compounds. Heterocycles are the largest and most diverse family of organic compounds. Among numerous nitrogen-containing heterocyclic compounds, imidazole is a key heterocyclic molecule in many biologically active compounds and synthetic drugs (13, 14).

We focus on developing an environmentally friendly method to synthesize substituted imidazole derivatives under mild conditions without producing hazardous by-products. The purpose of this study is to synthesize 2,4,5-trisubstituted imidazole derivatives in the presence of recyclable solid acid catalyst SiO_2PrOPDA-SO_4H.

2. EXPERIMENTAL SECTION

2.1. General Information

The rice husks were taken from Abbasiya town in Najaf City. All chemicals and solvents are purchased from BDH Sigma/Aldrich and Scharlau. The FTIR characterization was obtained by spectrophotometer 8400s Shimadzu, ranging from 4000 to 400 cm^{-1}. powder X-ray diffractometer was recorded by Philips PW 1730/10, which is equipped with a Cu-K_α source of radiation. Elemental analysis (CHNS) was performed by an Eager 300 computer on the EA1112. Scanning electron microscopy (SEM) was obtained by FESEM MIRA III (TESCAN)/(Czech Republic). Atomic force microscopy (AFM) was obtained by NT-MDT/INTEGRA (Nederland), and Thermogravimetric analysis was carried out on TA Instruments SDT- Q600, Belgium, from 30 to 900 °C at a heating rate of 20 °C per minute under nitrogen flow. ^{1}H NMR spectra were recorded on a Bruker 400 MHz German NMR spectrometer using DMSO-d_6 as the solvent, and TMS was employed as the internal standard. Mass spectra were obtained using an Agilent 5375 mass spectrometer.

2.2. Synthesis of the Catalyst

2.2.1. The preparation process of rice husks

The rice husk (RH) was washed two times in distilled water and left at room temperature for two days. 30 g of cleaned rice husk was added to the 500 mL of 1 M nitric acid and stirred at room temperature for 24 h. After that, the RH was washed with distilled water until it reached pH 6-7 and dried in an oven at 110 °C overnight. Rice husks, after this process, are labeled as RH-NO_3.

2.2.2. Preparation of sodium silicate solution from rice husks

The preparation process of the sodium silicate from RH-NO_3 was performed using a recently reported method (14, 15). 30 g of RH-NO_3 was mixed with 200 mL of 1 M sodium hydroxide in a plastic container and stirred for 24 h. The mixture was filtered to remove the residual cellulose. The filtration represented sodium silicate and was used as a precursor to the synthesis catalyst, as shown in Scheme 1.

2.2.3. Preparation of rice husk silica-3-(Chloropropyl)triethoxysilane (RH-SiO_2PrCl)

About 6 mL of 3-(chloropropyl)triethoxysilane (CPTES) was added to 50 mL of prepared sodium silicate solution. The mixture was titrated with 3 M HNO_3 until the pH reached 3. The formed gel was separated by centrifuge at 4000 r/min for 5 min. The mixture was washed with distilled water five times and finally washed with acetone, then dried at 110 °C for 24 h. The weight of the product was 6.4 g, and the prepared sample was labeled as RH-SiO_2PrCl, as shown in Scheme 1.

2.2.4. Preparation of acid catalyst (RH-SiO_2PrOPDA-SO_4H)

A 1 g of RH-SiO_2PrCl was added to the mixture of 2 g, 18.5 mmol *o*-phenylenediamine, and 2.6 mL, 18.8 mmol triethylamine in 30 mL of toluene. The mixture was refluxed at 110 °C for 24 h. The resulting solution contained a yellow solid precipitate, and it was filtered and washed with DMSO, ethanol, and acetone. Then dry at 110 °C for 24 h. Finally, 0.7 g of powder, which was RH-SiO_2PrOPDA, was collected. 40 mL of 0.5 M sulfuric acid was then stirred with (0.7 g) of the product at room temperature for 24 h., and the precipitate was washed with a large amount of distilled water and dried in an oven at 110 °C for 24 h. Finally, brown powder (1.20 g) was obtained, and the product was labeled as RH-SiO_2PrOPDA-SO_4H. As shown in Scheme 1.

2.3. Synthesis of 2,4,5-trisubstituted Imidazole Derivatives (4a-e)

A mixture of (1 mmol) benzil, (1 mmol) aldehyde, (5 mmol) ammonium acetate, and (0.04 g) RH-SiO_2PrOPDA-SO_4H was dissolved in (5 mL) ethanol. The mixture was heated to reflux and stirred for 4 h. After the reaction was completed, the crude product was poured into dichloromethane (10 mL), stirred for 15 min, then the solid Bronsted acid catalyst was removed by filtration. The catalyst was recovered in three consecutive cycles under the same conditions (Figure 13). Pour the filtrate into 10 mL of cold water and stir for 10 min. The precipitate was filtered, washed with water, and then dried under a vacuum. The product was purified by recrystallization in an ethanol-water mixture to give the 2,4,5-trisubstituted imidazole derivative, as shown in Scheme 2. All products were confirmed through melting point, FT-IR, ^{1}H NMR, and mass spectrometry analyses.

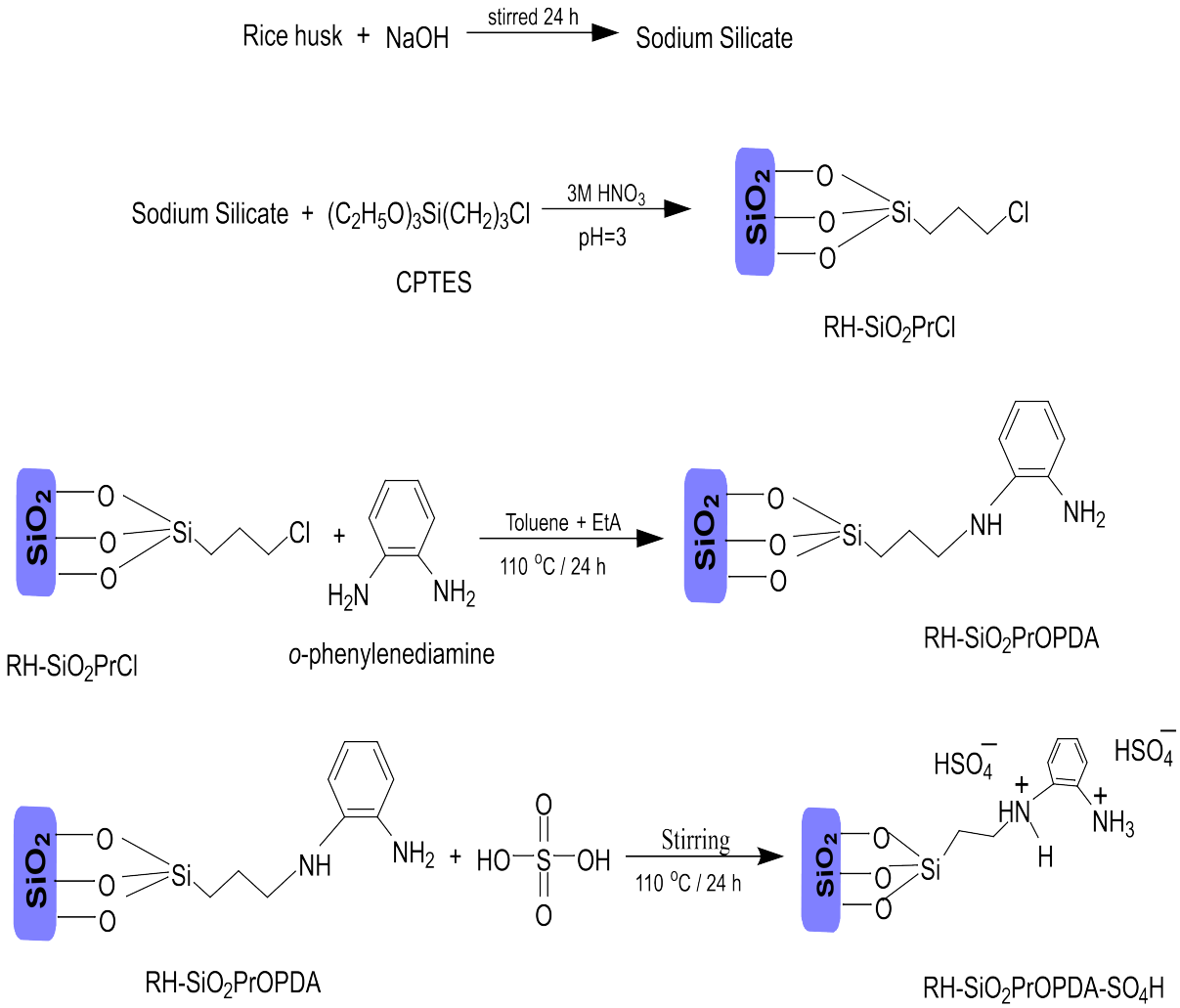

Scheme 1: Preparation process of RH-SiO_2PrOPDA-SO_4H.

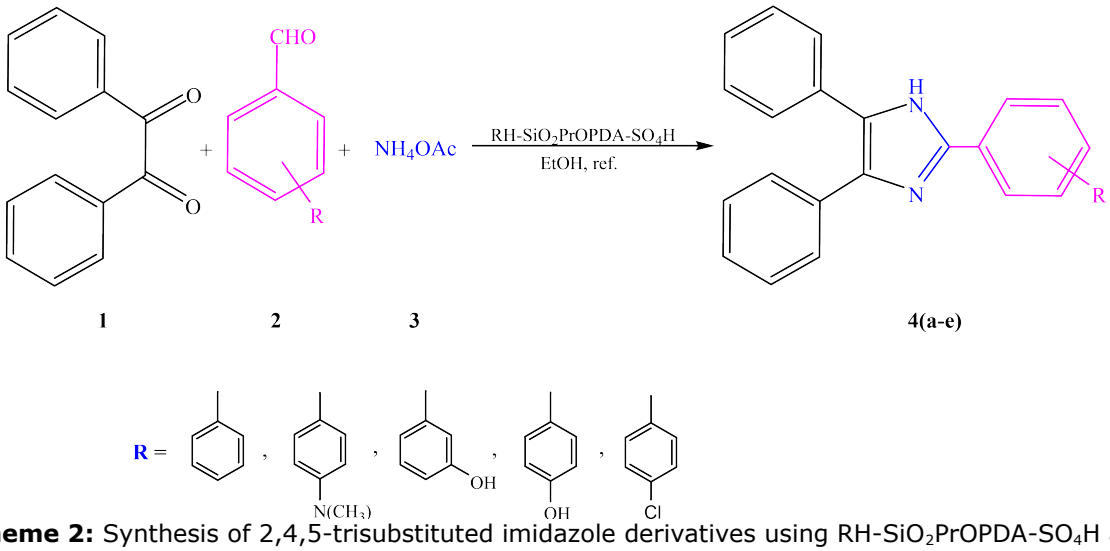

Scheme 2: Synthesis of 2,4,5-trisubstituted imidazole derivatives using RH-SiO_2PrOPDA-SO_4H as a catalyst.

2.4. Spectral Data for the Products

2,4,5-triphenylimidazole (**4a**): Yield: 99%; White solid; M.p. 267-269 °C (Lit. 267-269 °C) (16); IR (KBr) ῡ (cm^{-1}): 3315 (N–*H*), 3063 (Ar–*H*), 1662(*C*=*N*); ^{1}H NMR (400 MHz, DMSO-d_6) δ (ppm): 12.79 (s, N–*H*), 8.10 (d, *J* = 8.0 Hz, 2H, Ar–*H*), 7.57 – 7.54 (m, 3H, Ar–*H*), 7.52 – 7.33 (m, 8H, Ar–*H*), 7.29 – 7.21 (m, 2H, Ar–*H*); MS (ESI): m/z = 296.2 [M^+].

4-(4,5-diphenylimidazol-2-yl)-N,N-dimethylaniline (**4b**): Yield: 74%; light yellow solid; M.p. 234-236 °C (Lit. 234-236 °C) (17); 3480 (N–*H*), 3059 (Ar–*H*), 2939, 2866 and 2800 (C–*H*), 1612(*C*=*N*); ^{1}H NMR (400 MHz, DMSO-d_6) δ (ppm): 12.31 (s, N–*H*), 7.90

(d, *J* = 8.0 Hz, 2H, Ar–*H*), 7.50–7.20 (m, 10H, Ar–*H*), 6.79 (d, *J* = 8.0 Hz, 2H, Ar–*H*), 2.96 (s, 6H, N(CH_3)$_2$); MS (ESI): m/z = 339.4 [M^+].

3-(4,5-Diphenylimidazol-2-yl)phenol (**4c**): Yield: 71%; gray solid; M.p. 256–258 °C (Lit. 254–257 °C) (18); IR (KBr) ῡ (cm^{-1}): 3317 (O–*H*), 3190 (N–*H*), 3063 (Ar–*H*), 1666 (*C*=*N*); ^{1}H NMR (400 MHz, DMSO-d_6) δ (ppm): 12.61 (s, N–*H*), 9.56 (s, O–*H*), 7.55 – 7.49 (m, 5H, Ar–*H*), 7.44 (t, *J* = 8.0 Hz, 2H, Ar–*H*), 7.39 – 7.20 (m, 5H, Ar–*H*), 6.78 (d, *J* = 8.0 Hz, 2H, Ar–*H*); MS (ESI): m/z = 312.2 [M^+].

4-(4,5-diphenyl-1H-imidazol-2-yl)phenol (**4d**): Yield: 84%; beige solid; M.p. 232-235 °C (Lit. 233–236 °C) (19); IR (KBr) ῡ (cm^{-1}): 3313 (O–*H*), 3174 (N–*H*), 3032 (Ar–*H*), 1604 (*C*=*N*); ^{1}H NMR (400 MHz, DMSO-d_6) δ (ppm): 12.40 (s, N–*H*), 9.69 (s, O–*H*), 7.89 (d, *J* = 8.0 Hz, 2H, Ar–*H*), 7.53 (d, *J* = 8.0 Hz, 2H, Ar–*H*), 7.49 – 7.41 (m, 4H, Ar–*H*), 7.37 – 7.18 (m, 4H, Ar–*H*), 6.84 (d, *J* = 8.0 Hz, 2H, Ar–*H*); MS (ESI): m/z = 312.3 [M^+].

2-(4-chlorophenyl)-4,5-diphenylimidazole (**4e**): Yield: 44%; white solid; M.p. 258-261 °C (Lit. 257–260 °C) (20); IR (KBr) ῡ (cm^{-1}): 3182 (N–*H*), 3063 (Ar–*H*), 1666 (*C*=*N*); ^{1}H NMR (400 MHz, DMSO-d_6) δ (ppm): 12.69 (s, N–*H*), 8.08 (d, *J* = 8.0 Hz, 2H, Ar–*H*), 7.53–7.46 (m, 8H, Ar–*H*), 7.39–7.36 (m, 4H, Ar–*H*); MS (ESI): m/z = 330.3 [M^+].

3. RESULTS AND DISCUSSION

3.1. Fourier-Transform Infrared Spectroscopic Analysis (FT-IR)

Figure 1 shows the infrared spectrum of RH-SiO_2PrCl. The band near 3425 cm^{-1} is caused by the OH stretching vibration of silanol and water molecules adsorbed on the silica surface. Additionally, the band at 2958 cm^{-1} indicates the presence of CH stretching in the CH_2 propyl moiety (21, 22). The bending vibration of water molecules trapped in the silica matrix was detected as a strong peak at 1647 cm^{-1}. Moreover, bands at 1085, 698, and 462 cm^{-1} were assigned to the vibration modes of siloxane (Si-O-Si) (23, 24). A band at 698 cm^{-1} could be assigned to the chloro-carbon bond of the RH-SiO_2PrCl (25). These results indicate that CPTES was successfully incorporated into the silica matrix.

The FT-IR spectrum of the new catalyst RH-SiO_2PrOPDA-SO_4H in Figure 1 showed the presence of a band at 3433 cm^{-1}, indicating the presence of vibrations belonging to the N-H stretching group. Also, the band at 2947 cm^{-1} indicates the presence of a C-H stretching group vibration. The stretching vibration of the siloxane (Si-O-Si) appeared at 1111 cm^{-1}, which appeared at a higher frequency than compound RH-SiO_2PrCl. This indicated that the *o*-phenylenediamine was successfully immobilized onto RH-SiO_2PrCl. At the same point, the sulfuric acid functional group appears in the silica matrix with different absorption extents of the S=O stretching modes, which are located in the 1010-1080 cm^{-1} range, and the vibration band of S-O appears at 580 cm^{-1}. This indicates the success of stabilizing sulfonic acids (26) into the surfaces of RH-SiO_2PrOPDA-SO_4H.

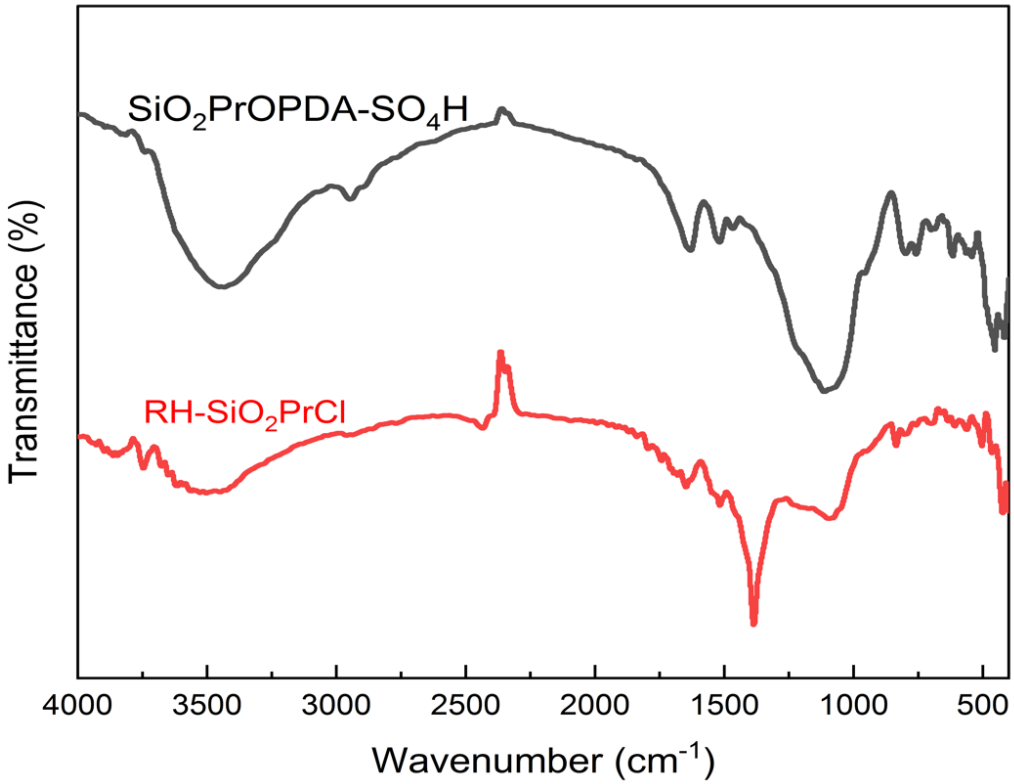

Figure 1: FT-IR analysis of RH-SiO_2PrCl and RH-SiO_2PrOPDA-SO_4H.

3.2. X-Ray Diffraction Analysis (XRD)

The XRD patterns of functionalized silica RH-SiO_2-PrCl and SiO_2PrOPDA-SO_4H show broad peaks at 2θ=2 in Figure 2, which indicates the amorphous structure of RH-SiO_2-PrCl and RH-SiO_2PrOPDA-SO_4H (27,28). However, no change occurred after fixation of *o*-phenylenediamine and sulfuric acid (29) on RH-SiO_2-PrCl in the new catalyst structure.

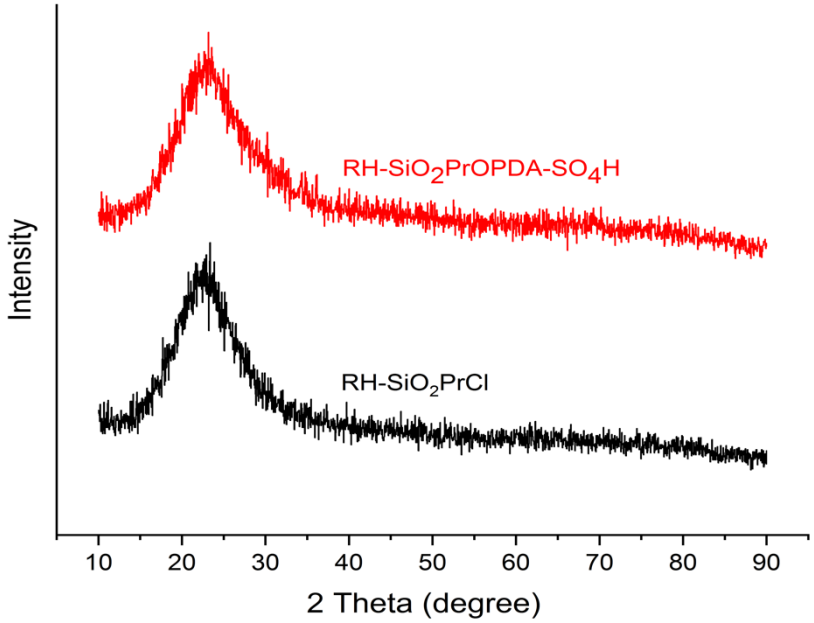

Figure 2: XRD analysis of RH-SiO_2PrCl and RH-SiO_2PrOPDA-SO_4H.

3.3. Nitrogen Adsorption Analysis

The specific surface area of the functionalized silica was 205.42 m^2/g, while for the new catalyst was 165 m^2/g. As a result, RH-SiO_2PrCl has a higher specific surface area caused by CPTES functioning as a directing agent for templates. This increase in porosity was attributed to the formation of a new structure of pores in the CPTES-silica composite (25). Adam and Andas (30) also reported similar findings. The reduction in surface area of the new catalyst is due to the acid treatment of the silica (31). In addition, the average pore diameters of RH-SiO_2PrCl and RH-SiO_2PrOPDA-SO_4H are 3.69 and 3.51 nm, respectively. The RH-SiO_2PrCl and RH-SiO_2PrOPDA-SO_4H samples exhibit type IV isotherms with an H3 hysteresis loop, which is typical of mesoporous solids. The pore size distribution is shown in the inset of Figure 3(a) and 3(b), where the pore size distribution is in the range of (5-20 nm) and belongs to mesoporous materials.

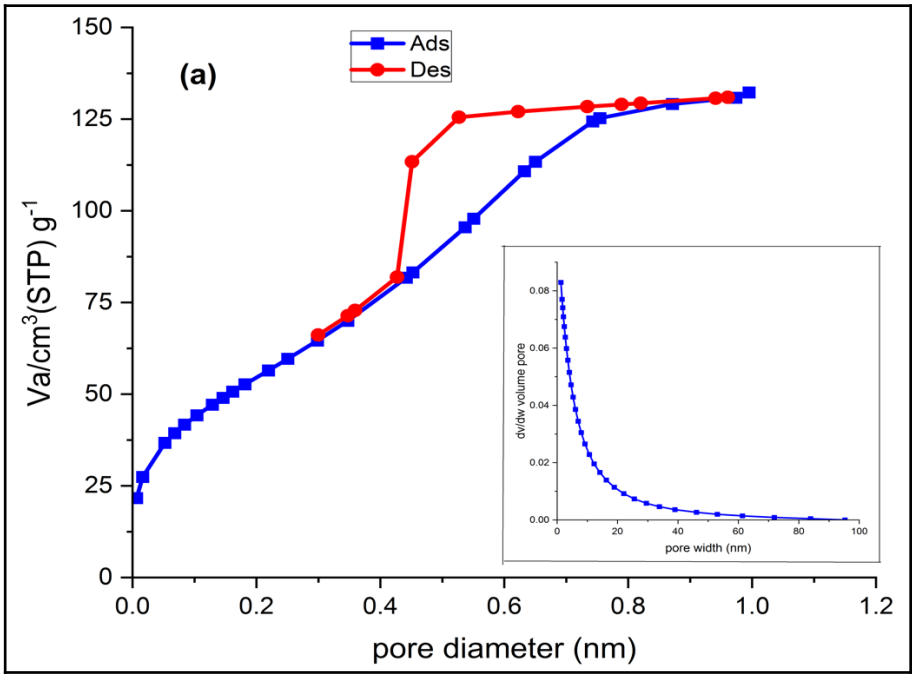

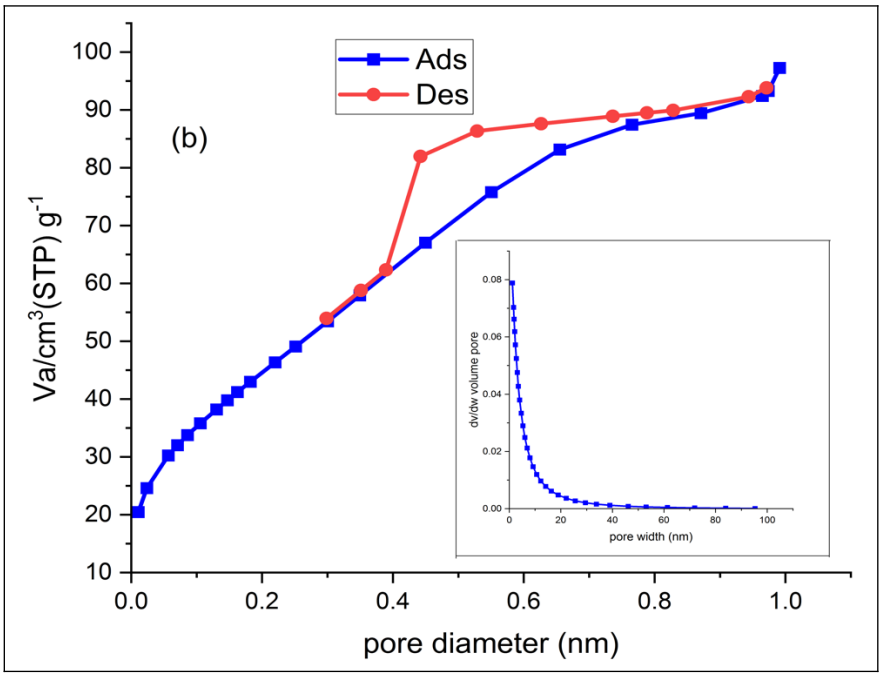

Figure 3: (a) N_2 adsorption–desorption isotherm and pore size distribution of RH-SiO_2PrCl. **(b)** N_2 adsorption–desorption isotherm and pore size distribution of RH-SiO_2PrOPDA-SO_4H.

3.4. Thermogravimetric Analysis (TGA)

The thermal stability of the samples of RH-SiO_2PrCl was evaluated by thermogravimetric analysis (TGA), and the weight loss observed was attributed to the degradation of the long-lasting components on the surface of the silica in Figure 4a. The results show that RH-SiO_2PrCl exhibits a weight change below 200 °C due to the loss of physically adsorbed water, and then experiences a stable weight loss below 600 °C, with decomposition weight loss increasing to 46% of the CPTES group in the matrix. At higher than 600°C, the silanol groups are converted into stable Si-O-Si siloxane bonds (32).

TGA analysis of RH-SiO_2PrOPDA-SO_4H (Figure 4(b)) shows a different type of decomposition than that of RH-SiO_2PrCl. The first decomposition occurs at temperatures below 300 °C due to water loss. In comparison, the second decomposition, start at temperatures between 300 and 600 °C, resulted in a weight loss of 65% due to the decomposition of the organic components immobilized on the catalyst surface. These results indicate that the acid catalyst is stable at the above temperatures.

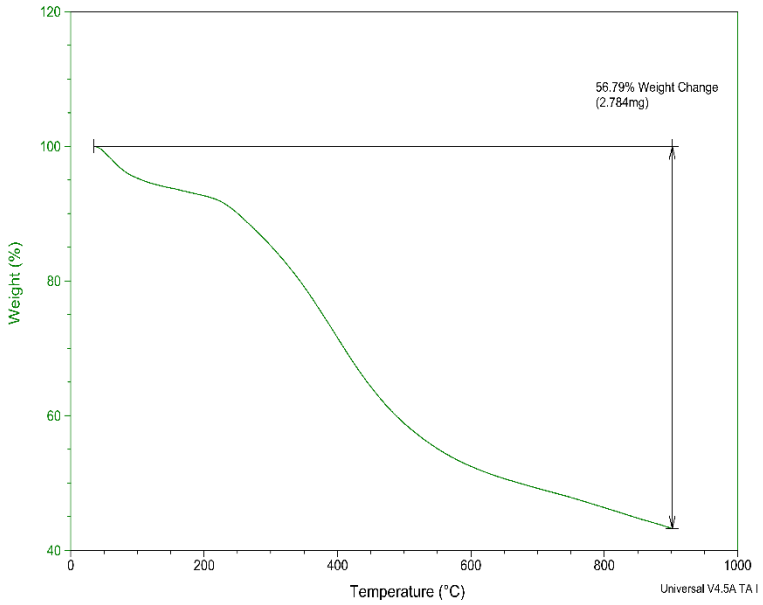

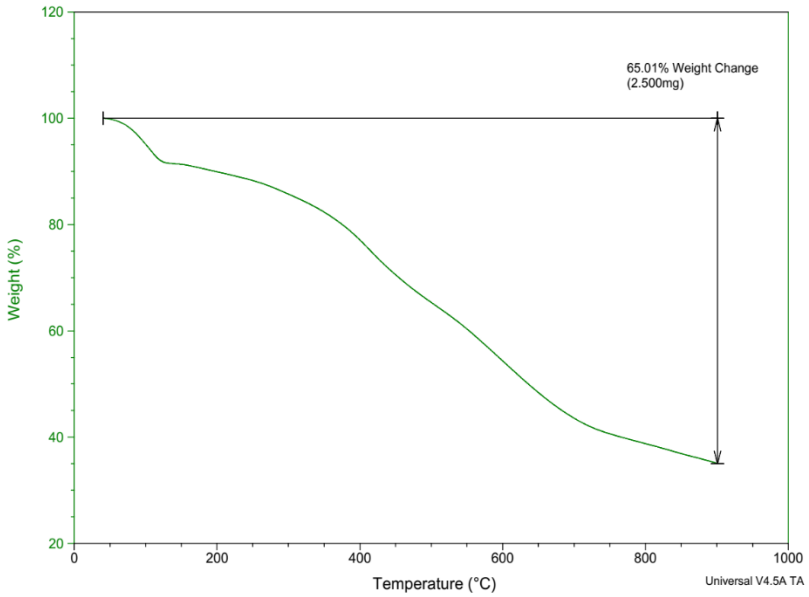

Figure 4: (a) TGA analysis of RH-SiO_2PrCl. **(b)** TGA analysis of RH-SiO_2PrOPDA-SO_4H.

3.5. Elemental Analysis (CHN)

The elemental analysis (CHNS) of the RH-SiO_2PrCl compound showed that the percentage of carbon and hydrogen reached 16.24% and 5.3%, respectively, as shown in Table 1. The elemental analysis of the RH-SiO_2PrOPDA-SO_4H compound indicated that the percentage of carbon, hydrogen, nitrogen, and Sulfur were 20.60%, 4.12%, 4%, and 3%, where the higher percentage of carbon, nitrogen, hydrogen, and Sulfur Results of treatment of functionalized silica with sulfuric acid and *o*-phenylenediamine.

Table 1: (CHNS) of the RH-SiO_2PrCl and RH-SiO_2PrOPDA-SO_4H.

Sample	C (%)	H (%)	N (%)	S (%)
RH-SiO_2PrCl	16.24	5.30	-	-
RH-SiO_2PrOPDA-SO_4H	20.60	5.12	4.00	3.00

3.6. Scanning Electron Microscopy–Energy Dispersive X-Ray (SEM/EDX)

FESEM analysis shows that RH-SiO_2PrCl in Figure 5 has a porous surface. In the FESEM image, the particles have irregular shapes. EDS analysis shows the presence of silicon, carbon, and oxygen in RH-SiO_2PrCl. The high carbon and oxygen content of silica in EDX analysis indicates the successful incorporation of CPTES into the silica matrix.

FESEM microscopic images of the new catalyst SiO_2PrOPDA-SO_4H are also shown in Figure 7. The surfaces were less porous than those of the functionalized silica (33), and EDS analysis is shown in Figure 8. The EDS spectrum showed peak oxygen density at 35.78%, carbon at 29.68%, silicon at 16.93%, nitrogen at 11.36%, and sulfur at 6.25. The increase in the percentage of these elements for the new catalyst indicates the succeeding incorporation of *o*-phenylenediamine with RH-SiO_2PrCl and sulfuric acid (34).

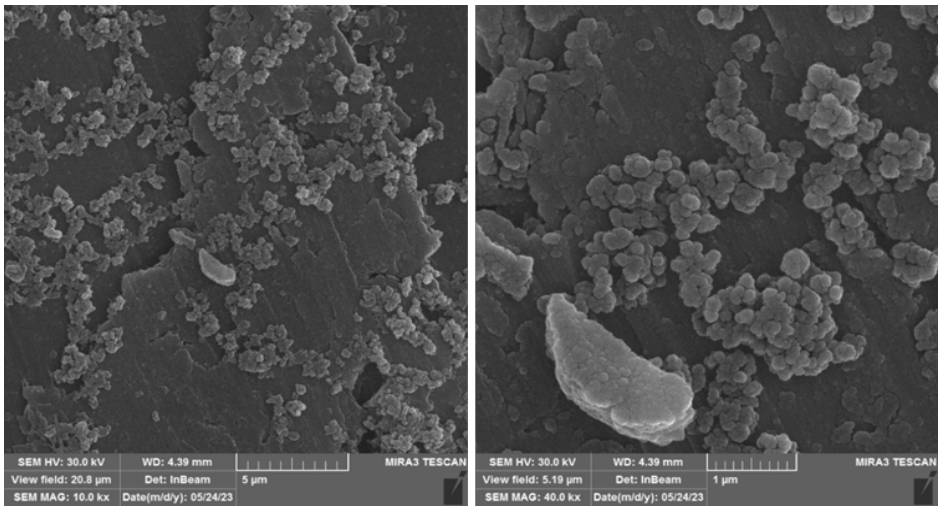

Figure 5: FESEM analysis of RH-SiO_2-PrCl.

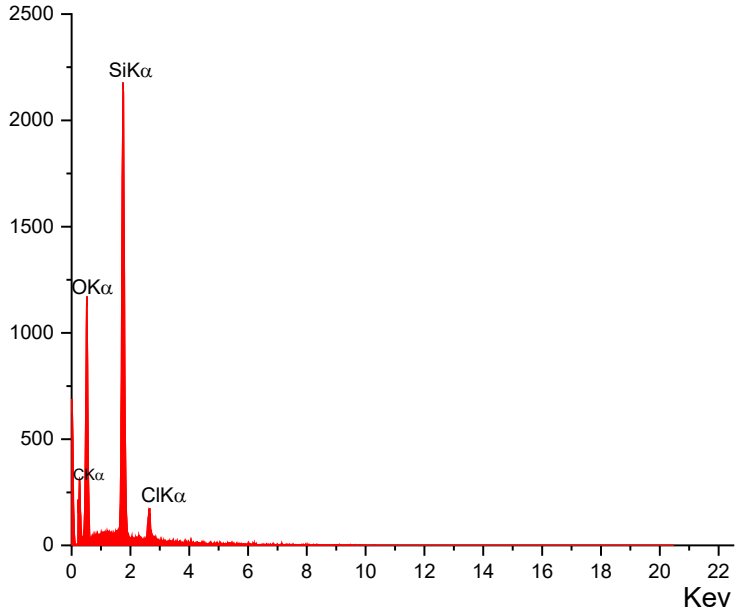

Figure 6: EDS analysis of RH-SiO_2PrCl.

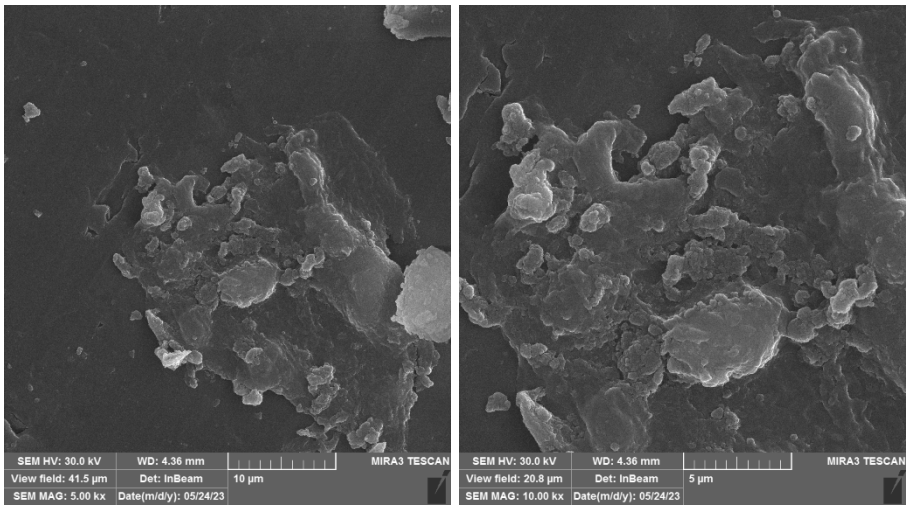

Figure 7: FESEM analysis of SiO_2PrOPDA-SO_4H.

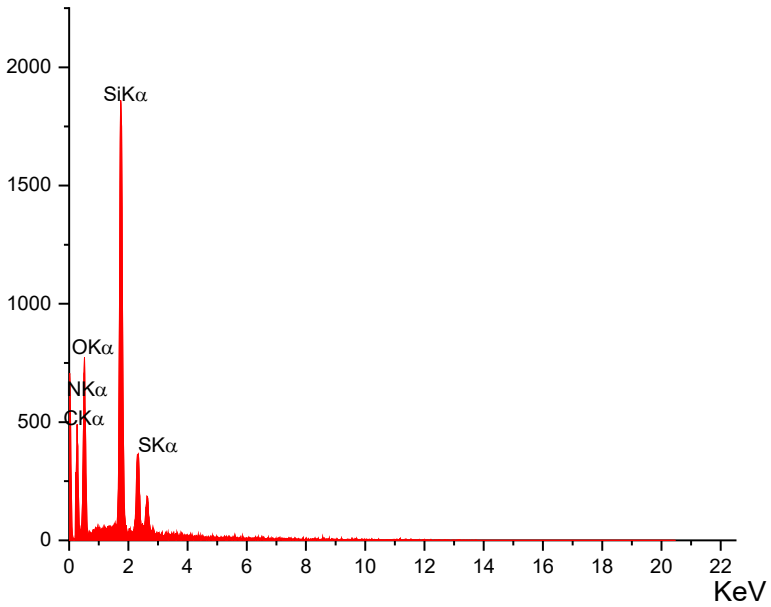

Figure 8: EDS analysis of SiO_2PrOPDA-SO_4H.

3.7. Atomic Force Microscopy (AFM)

The atomic force microscopy (AFM) images of RH-SiO_2PrCl and RH-SiO_2PrOPDA-SO_4H are shown in Figures 9 and 10, respectively. The structures appear pyramidal and irregular surfaces form. From comparing Figures 9 and 10, that note the surface of RH-SiO_2PrOPDA-SO_4H was less porous than functionalized silica RH-SiO_2-PrCl (35) due to add CPTES to silica. The estimated average roughness modulus (Ra) is 1.915 nm, and the root mean square roughness (Rrms) is 1.363 nm for the RH-SiO_2PrOPDA-SO_4H catalyst, which is larger than the roughness modulus and root square roughness of RH-SiO_2PrCl, 1.295 nm, and 845 pm, respectively. This change could be attributed to the successful modification the surface in RH-SiO_2PrCl by *o*-phenylenediamine and sulfuric acid.

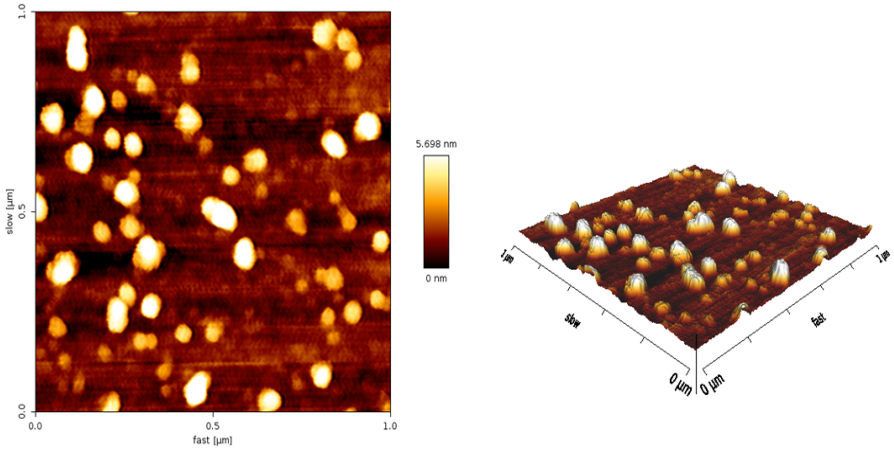

Figure 9: AFM 2D (in left) and 3D (in right) micrographs of RH-SiO_2PrCl.

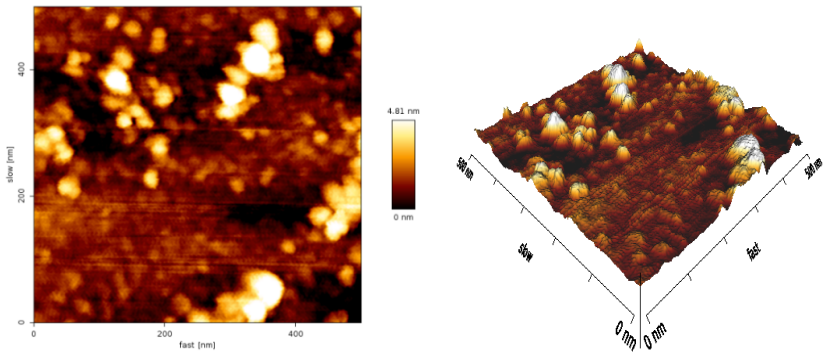

Figure 10: AFM 2D (in left) and 3D (in right) micrographs of RH-SiO_2PrOPDA-SO_4H.

3.8. Analysis with Transmission Electron Microscopy (TEM)

TEM microscopic images of RH-SiO_2PrCl functionalized silica shows spherical particles measuring between 10-15 nm. However, the particles are irregularly shaped, and visible porosity lines appear aligned, indicating the presence of a porous structure. This leads to a high surface area of RH-SiO_2PrCl functional silica (25, 36). As for the catalyst RH-SiO_2PrOPDA-SO_4H, the particle size is between 5-10 nm, and the distribution of particles could be seen with less dispersion than functional silica RH-SiO_2PrCl, and this indicates a decrease in the surface area due to the treatment of the functional silica with sulfuric acid.

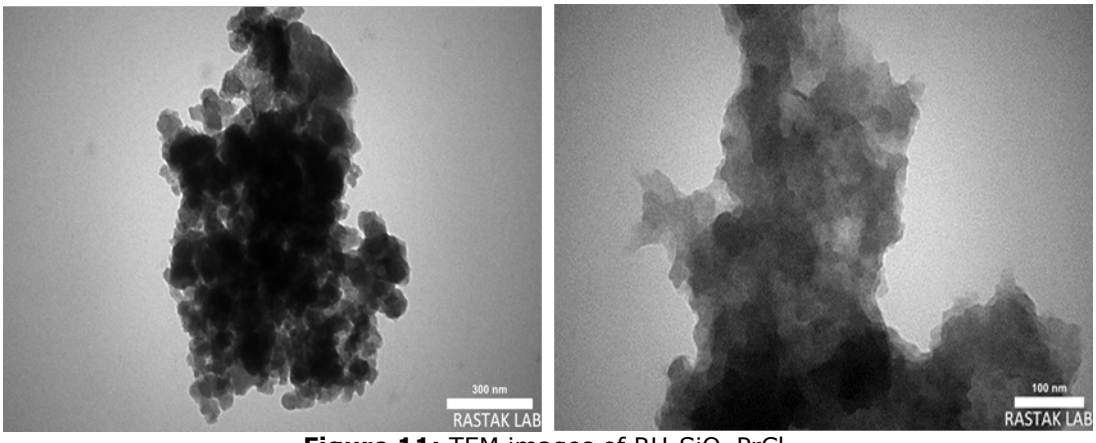

Figure 11: TEM images of RH-SiO_2PrCl.

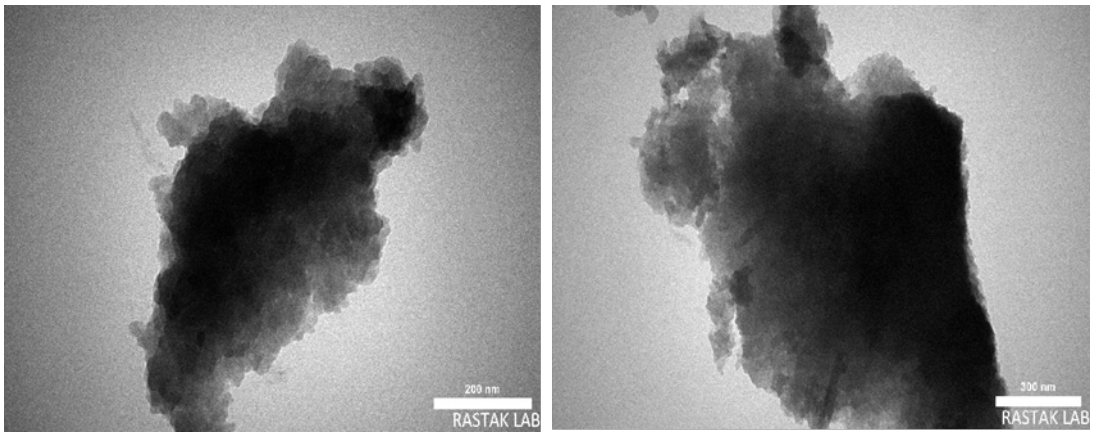

Figure 12: TEM images of RH-SiO_2PrOPDA-SO_4H.

3.9. Optimization of Reaction Conditions for Synthesis of 2,4,5-trisubstituted Imidazole Derivatives

The response between benzaldehyde, ammonium acetate, and benzil were selected as an example of a reaction that is intended to be studied (**4a**). The most effective conditions (Scheme 3) were determined as a result. Several different solvents and various molar ratios were examined for this process. The findings are listed in Tables 2 and 3. The highest yield percentage was achieved using ethanol as the solvent (Table 2, entry 3). The molar ratio demonstrated that the most effective and practical choice for the reaction was 1:1:5 (Table 3, entry 5). Additionally, the model reaction (**4a**) was conducted with different amounts of catalyst (Table 4). The highest percentage product was achieved when 0.04 g of catalyst was employed. (Table 4, entry 3). After successfully optimizing the reaction conditions, a series of 2,4,5-trisubstituted imidazole derivatives (**4a-e**) were prepared.

The spectral analyses of synthesized products were confirmed by comparison with those reported in the literature, and melting points were also recorded and compared with known compounds (16-20). ^{1}H NMR spectra exhibited the N–H proton of the imidazole ring in the downfield region, while FTIR spectra of the compounds (**4a-e**) showed packs at 3182–3480 and 1604–1666 cm^{-1} for the (N–H) and (C=N) groups, respectively.

Table 2: Effect of solvent on the synthesis of 2,4,5-triphenyl-1*H*-imidazole (**4a**).

Entry	Solvent	Yield %
1	H_2O	35
2	Methanol	46
3	Ethanol	99
4	CH_3CN	28
5	THF	71

Table 3: Effect of mole ratio on the synthesis of 2,4,5-triphenyl-1*H*-imidazole (**4a**).

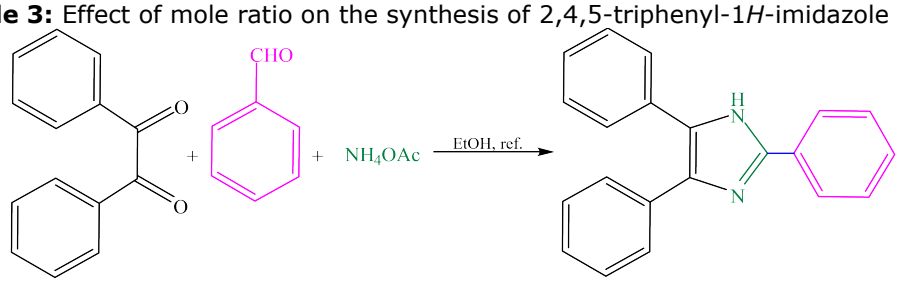

A B C

Entry	Mole ratio (A:B:C)	Yield %
1	1:1:1	92
2	1:1:2	39
3	1:1:3	42
4	1:1:4	96
5	1:1:5	99

Table 4: Effect of the catalyst amount on the synthesis of 2,4,5-triphenyl-1*H*-imidazole (**4a**).

Entry	Catalyst	Yield %
1	0.01	56
2	0.02	78
3	0.04	99
4	0.08	35
5	0.16	53

3.10. Reusability of the Catalyst

The benefit of using a new catalyst (RH-SiO_2PrOPDA-SO_4H) lies in its reusability, making it both environmentally friendly and cost-effective. To investigate the catalyst's recyclability, selected typical reactions were examined under identical optimized conditions. After each reaction, the catalyst was easily separated from the mixture by filtration and washed with dichloromethane. The dried catalyst was then retested for three consecutive cycles (Figure 13).

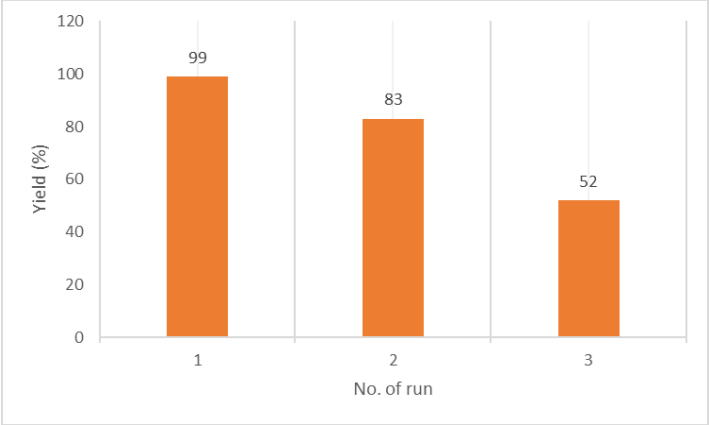

Figure 13: Reusability of the catalyst.

4. CONCLUSION

Based on some physical measurements, such as infrared spectra, nitrogen absorption analysis, and elemental analysis, it was found that *o*-phenylenediamine was functionalized on the RH-SiO_2PrCl to prepare RH-SiO_2PrOPDA. Then, amine groups in RH-SiO_2PrOPDA were sulfonated by a simple reaction with diluted sulfuric acid to prepare RH-SiO_2PrOPDA-SO_4H. After the sulfonation process, the SO_2 functional groups were clearly shown in the catalyst's FT-IR. BET measurements showed the fixation of a 3-(chloropropyl)triethoxysilane molecule on the silica surface, which increased the specific surface area of RH-SiO_2PrCl. An efficient approach with a simple work-up and mild reaction condition procedure for preparation of 2,4,5-trisubstituted imidazole derivatives *via* condensation of ammonium acetate as an ammonia source, various aldehydes and benzil in ethanol as better solvent was presented, by using RH-SiO_2PrOPDA-SO_4H as the recyclable and inexpensive catalyst. The easy synthesis, safer reaction conditions, and reusable catalyst several times are the highlights of this procedure.

5. CONFLICT OF INTEREST

The authors have no relevant financial or non-financial interests to disclose.

6. ACKNOWLEDGMENTS

The authors are thankful to the Department of Chemistry, College of Science, University of Kerbala, for providing the laboratory facility.

7. REFERENCES

1. Oluseun Adejumo I, Adebukola Adebiyi O. Agricultural solid wastes: Causes, effects, and effective management. In: Strategies of Sustainable Solid Waste Management [Internet]. IntechOpen; 2021. Available from: <URL>.

2. Siddique R, Cachim P. Waste and supplementary cementitious materials in concrete [Internet]. Waste and Supplementary Cementitious Materials in Concrete: Characterisation, Properties and Applications. Elsevier; 2018. 621 p. Available from: <URL>.

3. López-Alonso M, Martín-Morales M, Martínez-Echevarría MJ, Agrela F, Zamorano M. Residual biomasses as aggregates applied in cement-based materials. In: Waste and Byproducts in Cement-Based Materials [Internet]. Elsevier; 2021. p. 89–137. Available from: <URL>.

4. Phonphuak N, Chindaprasirt P. Types of waste, properties, and durability of pore-forming waste-based fired masonry bricks. In: Eco-Efficient Masonry Bricks and Blocks [Internet]. Elsevier; 2015. p. 103–27. Available from: <URL>.

5. Gnanamanickam SS. Rice and its importance to human life. In: Biological Control of Rice Diseases [Internet]. Dordrecht: Springer Netherlands; 2009. p. 1–11. Available from: <URL>.

6. Sangwan S, Singh R, Gulati S, Rana S, Punia J, Malik K. Solvent-free rice husk mediated efficient approach for synthesis of novel imidazoles and their

In vitro bio evaluation. Curr Res Green Sustain Chem [Internet]. 2022 Jan 1;5:100250. Available from: <URL>.

7. Lima SPB de, Vasconcelos RP de, Paiva OA, Cordeiro GC, Chaves MR de M, Toledo Filho RD, et al. Production of silica gel from residual rice husk ash. Quim Nova [Internet]. 2011;34(1):71–5. Available from: <URL>.

8. Ali HH, Hussein KA, Mihsen HH. Antimicrobial applications of nanosilica derived from rice grain husks. Silicon [Internet]. 2023 Aug 25;15(13):5735–45. Available from: <URL>.

9. Eshghi H, Hassankhani A. One-pot efficient beckmann rearrangement of ketones catalyzed by silica sulfuric acid. J Korean Chem Soc [Internet]. 2007 Aug 20;51(4):361–4. Available from: <URL>.

10. Riego JM, Sedin Z, Zaldívar J, Marziano NC, Tortato C. Sulfuric acid on silica-gel: An inexpensive catalyst for aromatic nitration. Tetrahedron Lett [Internet]. 1996 Jan 22;37(4):513–6. Available from: <URL>.

11. Manna J, Roy B, Sharma P. Efficient hydrogen generation from sodium borohydride hydrolysis using silica sulfuric acid catalyst. J Power Sources [Internet]. 2015 Feb 1;275:727–33. Available from: <URL>.

12. Adam F, Hello KM, Ali TH. Solvent free liquid-phase alkylation of phenol over solid sulfanilic acid catalyst. Appl Catal A Gen [Internet]. 2011 May 31;399(1–2):42–9. Available from: <URL>.

13. Tolomeu HV, Fraga CAM. Imidazole: Synthesis, functionalization and physicochemical properties of a privileged structure in medicinal chemistry. Molecules [Internet]. 2023 Jan 13;28(2):838. Available from: <URL>.

14. Ali HH, Mihsen HH, Hussain KA. Synthesis, characterization and antimicrobial studies of modified silica materials derived from rice husks. Bionanoscience [Internet]. 2023 Sep 28;13(3):1163–76. Available from: <URL>.

15. Tariq A, Mihsen HH, Saeed SI. Organic–inorganic hybrid modified silica synthesized from rice husks straw for effective uptake of Co(II), Ni(II), and Cu(II) ions from aqueous solutions. Biomass Convers Biorefinery [Internet]. 2023 Dec 28;1:1–13. Available from: <URL>.

16. Samai S, Nandi GC, Singh P, Singh MS. L-Proline: An efficient catalyst for the one-pot synthesis of 2,4,5-trisubstituted and 1,2,4,5-tetrasubstituted imidazoles. Tetrahedron [Internet]. 2009 Dec 5;65(49):10155–61. Available from: <URL>.

17. Noriega-Iribe E, Díaz-Rubio L, Estolano-Cobián A, Barajas-Carrillo VW, Padrón JM, Salazar-Aranda R, et al. In vitro and In silico screening of 2,4,5-Trisubstituted imidazole derivatives as potential xanthine oxidase and acetylcholinesterase inhibitors, antioxidant, and antiproliferative agents. Appl Sci [Internet]. 2020 Apr 22;10(8):2889. Available from: <URL>.

18. Ahmed NS, Hanoon HD. A green and simple method for the synthesis of 2,4,5-trisubstituted-1H-imidazole derivatives using acidic ionic liquid as an effective and recyclable catalyst under ultrasound. Res Chem Intermed [Internet]. 2021 Oct 19;47(10):4083–100. Available from: <URL>.

19. Hilal DA, Hanoon HD. Bronsted acidic ionic liquid catalyzed an eco-friendly and efficient procedure for synthesis of 2,4,5-trisubstituted imidazole derivatives under ultrasound irradiation and optimal conditions. Res Chem Intermed [Internet]. 2020 Feb 27;46(2):1521–38. Available from: <URL>.

20. Hanoon HD, Radhi SM, Abbas SK. Simple and efficient synthesis of 2,4,5-triarylsubstituted imidazole derivatives via a multicomponent reaction using microwave irradiation. In: AIP Conference Proceedings [Internet]. American Institute of Physics Inc.; 2019. p. 020005. Available from: <URL>.

21. Hello KM, Ibrahim AA, Shneine JK, Appaturi JN. Simple method for functionalization of silica with alkyl silane and organic ligands. South African J Chem Eng [Internet]. 2018 Jun 1;25:159–68. Available from: <URL>.

22. Mihsen HH, Rfaish SY, Abass SK, Sobh HS. Synthesis and characterization of silica-thioamide hybrid compounds derived from rice husk ash with expected biological and catalytic activity. J Glob Pharma Technol [Internet]. 2018;10(11):590–8. Available from: <URL>.

23. Saravanan S, Dubey RS. Synthesis of SiO_2 nanoparticles by sol-gel method and their optical and structural properties. Rom J Inf Sci Technol [Internet]. 2020;23(1):105–12. Available from: <URL>.

24. Abbas SK, Hassan ZM, Mihsen HH, Eesa MT, Attol DH. Uptake of nickel(II) ion by Silica-o-Phenylenediamine derived from rice husk ash. Silicon [Internet]. 2020 May 18;12(5):1103–10. Available from: <URL>.

25. Adam F, Osman H, Hello KM. The immobilization of 3-(chloropropyl)triethoxysilane onto silica by a simple one-pot synthesis. J Colloid Interface Sci [Internet]. 2009 Mar 1;331(1):143–7. Available from: <URL>.

26. Elzanati E, Abdallah H, Farg E, Ettouney RS. Enhancing the esterification conversion using pervaporation. J Eng Sci Technol [Internet]. 2018;13(4):990–1004. Available from: <URL>.

27. Adam F, Hello KM, Osman H. Esterification via saccharine mediated silica solid catalyst. Appl Catal A Gen [Internet]. 2009 Aug 31;365(2):165–72. Available from: <URL>.

28. Sobh HS, Mihsen HH. Synthesis of functionalized silica from rice husks containing C-I end group. Baghdad Sci J [Internet]. 2019 Dec 1;16(4):886–91. Available from: <URL>.

29. Vijayalakshmi U, Vaibhav V, Chellappa M, Anjaneyulu U. Green synthesis of silica nanoparticles and its corrosion resistance behavior on mild steel. J Indian Chem Soc. 2015;92(5):675–8.

30. Adam F, Andas J. Amino benzoic acid modified silica—An improved catalyst for the mono-substituted product in the benzylation of toluene with benzyl chloride. J Colloid Interface Sci [Internet]. 2007 Jul 1;311(1):135–43. Available from: <URL>.

31. Esmaili S, Khazaei A, Ghorbani-Choghamarani A, Mohammadi M. Silica sulfuric acid coated on $SnFe_2O_4$ MNPs: Synthesis, characterization and catalytic applications in the synthesis of polyhydroquinolines. RSC Adv [Internet]. 2022 May 12;12(23):14397–410. Available from: <URL>.

32. Permatasari N, Sucahya TN, Dani Nandiyanto AB. Review: Agricultural wastes as a source of silica material. Indones J Sci Technol [Internet]. 2016 Apr 1;1(1):82. Available from: <URL>.

33. Nah HY, Parale VG, Jung HNR, Lee KY, Lim CH, Ku YS, et al. Role of oxalic acid in structural formation of sodium silicate-based silica aerogel by ambient pressure drying. J Sol-Gel Sci Technol [Internet]. 2018 Feb;85(2):302–10. Available from: <URL>.

34. Guedes R, Prosdocimi F, Fernandes G, Moura L, Ribeiro H, Ortega J. Amino acids biosynthesis and nitrogen assimilation pathways: A great genomic deletion during eukaryotes evolution. BMC Genomics [Internet]. 2011 Dec 22;12(S4):S2. Available from: <URL>.